Dynamic mechanical relaxation behavior of $Zr_{35}Hf_{17.5}Ti_{5.5}Al_{12.5}Co_{7.5}Ni_{12}Cu_{10}$ high entropy bulk metallic glass

L.T. Zhang[a], Y.J. Duan[a], T. Wada[b], H. Kato[b], J.M. Pelletier[c], D. Crespo[d], E. Pineda[d], J.C. Qiao[a,*]

[a] *School of Mechanics, Civil Engineering and Architecture, Northwestern Polytechnical University, Xi'an 710072, China*

[b] *Institute for Materials Research, Tohoku University, Sendai 980-8577, Japan*

[c] *Université de Lyon, MATEIS, UMR CNRS5510, Bat. B. Pascal, INSA-Lyon, F-69621 Villeurbanne Cedex, France*

[d] *Department of Physics, Barcelona Research Center in Multiscale Science and Technology, Institute of Energy Technologies, Universitat Politècnica de Catalunya, 08019, Barcelona, Spain*

* Corresponding author: Prof. Dr. J.C. Qiao

Email: qjczy@nwpu.edu.cn

Abstract: Non-equiatomic high entropy bulk metallic glasses were reported recently and show unique mechanical and physical properties. Dynamic mechanical relaxation behavior of $Zr_{35}Hf_{17.5}Ti_{5.5}Al_{12.5}Co_{7.5}Ni_{12}Cu_{10}$ high entropy bulk metallic glass was investigated by dynamic mechanical analysis (DMA) and the mechanical spectra could be well described by the quasi-point defects (QPD) theory. Compared to typical metallic glasses, the intensity of the β relaxation of $Zr_{35}Hf_{17.5}Ti_{5.5}Al_{12.5}Co_{7.5}Ni_{12}Cu_{10}$ high entropy bulk metallic glass is lower due to the sluggish diffusion. At the same time, the correlation factor χ is higher than that of conventional metallic glasses and this is ascribed to the high configuration entropy. In parallel, physical aging below the glass transition temperature leads to a decrease of atomic mobility, caused by a decrease of the concentration of defects.

Keywords: High entropy bulk metallic glass; Mechanical relaxation; Quasi-point defects; Physical aging

1. Introduction

Metallic glasses (MGs) and high entropy alloys (HEAs) have attracted extensive attention due to their special mechanical and physical properties. On the one hand, MGs are multicomponent alloys with inherent long-range disordered atomic structure prepared by rapid cooling methods [1, 2]. In the absence of the characteristic defects of crystalline materials, such as dislocations and grain boundaries, MGs possess superb (near the theoretical limit) strength, low elastic modulus and excellent corrosion resistance[3, 4]. On the other hand, HEAs are multicomponent alloys which contain at least five elements with equiatomic or near equiatomic (5~35 at.%) concentration[5] and a configuration entropy $S_c > 1.5R$, where R is the gas constant. The configuration entropy is defined as $S_c = -R\sum_{i=1}^{n} x_i \ln(x_i)$, where x_i is the concentration of the ith component[5]. HEAs show four main features, namely: high entropy, sluggish diffusion, cocktail effect and severe lattice distortion[6]. Overlapping the definitions of MGs and HEAs, high entropy metallic glasses have been developed in recent years[5, 7]. Aiming to maximize the S_c, equiatomic systems were first produced. Compared with the traditional metallic alloys, high entropy metallic glasses show unique mechanical and physical properties. Recent investigations proved that $Ti_{16.7}Zr_{16.7}Hf_{16.7}Cu_{16.7}Ni_{16.7}Be_{16.7}$ high entropy metallic glass shows high compressive strength at ambient temperature[7]. $Pd_{20}Pt_{20}Cu_{20}Ni_{20}P_{20}$ high entropy metallic glass presents excellent glass forming ability (GFA) with a critical diameter larger than 10 mm[8]. $Ca_{20}Mg_{20}Zn_{20}Sr_{20}Yb_{20}$ high entropy metallic glass has a potential application as a biomaterial[9]. It is already noted that high entropy metallic glasses are important candidates to be applied as functional and structural materials.

Regarding to configuration entropy, equiatomic high entropy metallic glasses such as $Pd_{20}Pt_{20}Cu_{20}Ni_{20}P_{20}$ will have highest configuration entropy S_c = $-R\cdot[\ln(0.2)\times 0.2\times 5]=1.61R$[8]. However, it has been recently reported that the highest configuration entropy is not always necessary to obtain convenient properties[10]. As a matter of fact, when the configuration entropy is higher than $1.5R$, the effect of configuration entropy becomes significant on the thermodynamics. One can achieve $S_c > 1.5\ R$ by adjusting the content of each component between 5 and 35 at.%. Considering as example an alloy such as $A_{30}B_{25}C_{20}D_{20}E_5$, the configuration entropy S_c = $-R\cdot[\ln(0.3)\times 0.3+\ln(0.25)\times 0.25+\ln(0.25)\times 0.25+\ln(0.2)\times 0.2+\ln(0.5)\times 0.5] = 1.501R$. From the perspective of entropy, an $A_{30}B_{25}C_{20}D_{20}E_5$ metallic glass is a new high entropy metallic glass. Compared to the equiatomic or near equiatomic alloy systems, non-

equiatomic high entropy metallic glasses show advantageous mechanical and physical properties due to the substitution of one element by another with a similar atomic radius[11]. The mixing enthalpy between the chemical composition and substituent elements is approximately equal to zero and, consequently, such substitution particularly affects the configuration entropy. Following this concept, the non-equiatomic $Zr_{35}Hf_{17.5}Ti_{5.5}Al_{12.5}Co_{7.5}Ni_{12}Cu_{10}$ high entropy bulk metallic glass (HEBMG) with excellent glass forming ability was developed [12]. The configuration entropy can be readily calculated as $S_c = -R\cdot[\ln(0.35)\times0.35+\ln(0.175)\times0.175+\ln(0.055)\times0.055+\ln(0.075)\times0.075+\ln(0.125)\times0.125+\ln(0.12)\times0.12+\ln(0.1)\times0.1]=1.77R$.

Mechanical relaxation processes are intrinsic attributes of glassy solids[13]. There are two main relaxation processes in glassy materials, i.e., main α relaxation and secondary β relaxation[2, 14]. The α relaxation is a thermodynamically irreversible process, corresponding to large scale atomic or molecular rearrangement. On the contrary, the β relaxation is a reversible process, which is related to local atomic rearrangement or molecular movement of the glassy materials[15]. It is well documented that the main α relaxation and secondary β relaxation processes are fundamental to understand the glass transition phenomenon, the diffusion behavior or the mechanical and physical properties of MGs[2, 16]. High entropy metallic glasses feature sluggish atomic diffusion together with excellent thermo-stability[17]. Therefore, high entropy metallic glasses are excellent model systems to investigate the mechanical dynamics (i.e. main α relaxation, secondary β relaxation) and mechanical properties (i.e. creep behavior, stress relaxation and plasticity).

According to previous literature, some investigations have reported the mechanical relaxation behavior of high entropy metallic glasses [18, 19]. Specifically, it is believed that high mixing entropy is beneficial to reduce the Gibbs free energy[20]. As a consequence, the high entropy effect has a favorable influence on GFA and mechanical properties of high entropy metallic glasses. It is well accepted that sluggish diffusion significantly hinders the atomic rearrangement of high entropy metallic glasses[21]. However, the dynamics of mechanical relaxation in high entropy metallic glasses, in particular, in non-equiatomic high entropy metallic glasses, is not clear yet. In the current work, the $Zr_{35}Hf_{17.5}Ti_{5.5}Al_{12.5}Co_{7.5}Ni_{12}Cu_{10}$ non-equiatomic HEBMG was chosen as the model alloy, in order to probe its dynamic mechanical relaxation behavior.

The experimental dynamic mechanical behavior was described in the framework of the quasi-point defects (QPD) physical model.

2. Experimental procedure

According to the literature, $Zr_{35}Hf_{17.5}Ti_{5.5}Al_{12.5}Co_{7.5}Ni_{12}Cu_{10}$ HEBMG shows an excellent GFA with a critical diameter of 18 mm[12]. In the current research, master alloy ingots were prepared by arc melting in a titanium-gettered argon atmosphere. In order to ensure the chemical homogeneity of the master alloy, the ingots were re-melted at least six times. $Zr_{35}Hf_{17.5}Ti_{5.5}Al_{12.5}Co_{7.5}Ni_{12}Cu_{10}$ HEBMG was prepared by the copper mould suction casting technique.

The amorphous nature of the as-cast sample was confirmed by X-ray diffraction (XRD, D8, Bruker AXS Gmbh) using Cu Kα radiation. Thermal properties, i.e., the glass transition temperature T_g and the crystallization onset temperature T_x, were determined by differential scanning calorimeter (DSC, Pekin Elmer, DSC 7) at a heating rate of 3 K/min.

The dynamic mechanical behavior of the model alloy was tested in a dynamic mechanical analyzer (DMA, TA instruments Q800) in single-cantilever bending mode. The dimension of the samples was around 30 mm (length)× 2 mm (width) × 1 mm (thickness). A sinusoidal stress $\sigma = \sigma_0\cos(2\pi f t)$ (f is the driving frequency) was applied to the materials, and the strain was recorded as $\varepsilon = \varepsilon_0\cos(2\pi f t + \delta)$. Here δ is the phase angle between the stress and strain, which depends on the material, driving frequency and temperature. The complex modulus of the material can be expressed as $E = \sigma/\varepsilon = E' + iE''$. E' is the storage modulus, which corresponds to the elastic response. E'' is the loss modulus, which is closely associated with the visco-elastic response. Note that $\tan\delta = E''/E'$ is defined as the loss factor (also called internal friction) of the material, which is linked to the mobility of the atoms or molecules of the glassy materials.

3. Results and discussion

Fig. 1 presents the DSC curve of $Zr_{35}Hf_{17.5}Ti_{5.5}Al_{12.5}Co_{7.5}Ni_{12}Cu_{10}$ HEBMG. The glass transition temperature T_g and the onset temperature of crystallization T_x, are indicated in **Fig. 1**. The inset exhibits the XRD pattern of the as produced $Zr_{35}Hf_{17.5}Ti_{5.5}Al_{12.5}Co_{7.5}Ni_{12}Cu_{10}$ HEBMG. No sharp peaks corresponding to crystalline phases were detected, which confirms the glassy nature of the alloy.

DMA is a powerful technique to probe the dynamic mechanical relaxation

processes of non-crystalline materials[2, 22]. **Fig. 2(a)** shows the evolution of the normalized storage modulus E'/E_u and the loss modulus E''/E_u of the $Zr_{35}Hf_{17.5}Ti_{5.5}Al_{12.5}Co_{7.5}Ni_{12}Cu_{10}$ HEBMG with temperature, determined at a frequency of 0.3 Hz and at a heating rate of 3 K/min. E_u is the value of the storage modulus at ambient temperature. Three distinct regions are observed:

(i) At low temperature, i.e., from ambient temperature to 500 K, the normalized storage modulus E'/E_u remains almost constant ($E'/E_u \sim 1$) and the loss modulus E''/E_u is close to zero. No viscoelastic effects are observed in this temperature range, where the mechanical behavior is dominated by the elastic response.

(ii) When the temperature ranges from 500 K to 770 K, the storage modulus decreases by increasing the temperature. On parallel, the loss modulus increases and reaches a maximum value around 751 K. This phenomenon corresponds to the main α relaxation of the glassy solids. The main α relaxation is connected with the glass transition of the amorphous materials. From T_g to T_x, glasses, including MGs, are staying in a metastable liquid state; this temperature range is called the supercooled liquid region (SLR). It is well accepted that MGs show excellent homogeneous flow (i.e. super-plasticity) in the SLR[23]. As a consequence, the deformation response of MGs transforms from non-Newtonian in the glass to Newtonian rheological deformation in the SLR[24].

(iii) When the temperature is above 770 K, the storage modulus and the loss modulus decrease again due to the formation of a crystalline phase.

There are typically two relaxation processes in glassy materials, i.e., the secondary slow β (also called Johari-Goldstein) relaxation and the main α relaxation[25]. **Fig. 2(b)** exhibits the normalized loss modulus E''/E''_{max} (E''_{max} is the maximum value of the loss modulus) of some typical MGs as a function of the normalized temperature T/T_α (T_α is the peak temperature of α relaxation). The intensity of β relaxation varies in different MGs. La-based MGs, such as $(La_{0.7}Ce_{0.3})_{65}Al_{10}Co_{25}$, show a prominent peak in the loss modulus corresponding to β relaxation while Zr-based MGs, such as $Zr_{56}Co_{28}Al_{16}$ or $Zr_{53}Al_{16}(Co_{0.75}Ag_{0.25})_{31}$, display a moderate secondary relaxation process often termed as "excess wing". The $Zr_{35}Hf_{17.5}Ti_{5.5}Al_{12.5}Co_{7.5}Ni_{12}Cu_{10}$ HEBMG studied in this work shows also an excess wing. It can be seen that the β relaxation process spans over a broad temperature range, from 0.65 T_α to about 0.8 T_α[16]. According to dielectric spectroscopy measurements, organic glasses show similar dielectric relaxation

processes[26]. It has been proved that slow β relaxation is closely correlated with the structural heterogeneity of MGs[2, 27]. In addition, the slow β relaxation is closely correlated to the diffusion of the smallest atoms among the species constituting the chemical composition of MGs[16]. It should be stressed that the intensity of the β relaxation of $Zr_{35}Hf_{17.5}Ti_{5.5}Al_{12.5}Co_{7.5}Ni_{12}Cu_{10}$ HEBMG is lower than that of typical MGs due to the sluggish diffusion of high entropy alloys.

It is well documented that mechanical relaxation behavior of MGs shows a strong frequency dependence[14, 28]. **Fig. 3** shows the normalized loss modulus as a function of the temperature with different driving frequencies (0.05-0.1-0.3-0.5 Hz). The peak temperature of the main α relaxation moves to high temperature region by increasing the driving frequency. In the frequency domain, the correlation between the characteristic temperature of the main α relaxation of the glass and the driving frequency of the mechanical excitation obeys a Vogel-Fucher-Tammann (VFT) equation[29]:

$$f = \kappa \exp\left(\frac{B}{T_0 - T_\alpha}\right) \tag{1}$$

where κ, B and T_0 are fitting parameters. In a narrow frequency window, the VFT equation can be approximately equivalent to the Arrhenius equation:

$$f = f0\exp\left(\frac{E\alpha}{k_B T\alpha}\right) \tag{2}$$

where $E\alpha$ is the apparent activation energy of the main α relaxation of glassy materials, k_B is the Boltzmann constant and $f0$ is a pre-factor. The inset of **Fig. 3** shows the linear correlation between the driving frequency and the peak temperature of the α relaxation. The apparent activation energy of the main α relaxation of $Zr_{35}Hf_{17.5}Ti_{5.5}Al_{12.5}Co_{7.5}Ni_{12}Cu_{10}$ HEBMG can be computed as E_α = 6.1 eV. The activation energy of the main α relaxation in the high entropy metallic glass is in good accordance with values observed in typical MGs[30].

The activation energy of the main α relaxation E_α and glass transition temperature T_g in typical MGs are listed in **Table 1** (experimental results of other MGs were obtained from the literature). **Fig. 4** shows the correlation between the activation energy of the α relaxation E_α and the glass transition temperature T_g for typical MGs, showing

a broad linear correlation. Although the empirical ratio of E_α to E_β is approximately 2~7[14], it sufficiently substantiates the physical prospect that β relaxation is a key underlying process controlling the α relaxation and the glass transition process. The correlation between β relaxation and α relaxation is of great significance for investigating the glass transition in MGs[2].

In order to well understand the dynamic mechanical properties of $Zr_{35}Hf_{17.5}Ti_{5.5}Al_{12.5}Co_{7.5}Ni_{12}Cu_{10}$ HEBMG, the isothermal frequency spectra of storage and loss moduli are shown in **Fig. 5(a)** and **(b)** in a wide temperature range (from 600 to 780 K, with an interval of 5 K). For temperatures below the glass transition temperature T_g, it can be seen that:

(i) At a given isothermal temperature, the storage modulus decreases by decreasing the frequency. At the same time, the loss modulus increases as the frequency decreases.

(ii) At a given frequency, the storage modulus decreases by increasing the temperature. In contrast, the loss modulus increases by increasing the temperature. It should be noted that the main α relaxation peak was not observed during the isothermal testing spectra due to the formation of the crystalline phase during the isothermal steps at temperatures around T_g, as it is reported in other MGs[18, 31].

On the basis of the time-temperature superposition (TTS) principle, master curves of the elastic moduli of glassy materials can be obtained within a large frequency domain by a simple horizontal shift; a given temperature is selected as a reference temperature T_{ref}. **Fig. 5(c)** shows the master curve readily obtained based on the isothermal frequency spectra of the normalized storage modulus and loss modulus of $Zr_{35}Hf_{17.5}Ti_{5.5}Al_{12.5}Co_{7.5}Ni_{12}Cu_{10}$ HEBMG. The loss modulus decreases while the storage modulus increases by increasing the frequency.

Both experimental evidence, numerical simulation and theoretical analysis verified that structural heterogeneity is an intrinsic feature of MGs[32, 33]. In essence, mechanical and physical properties of MGs are closely connected to the structural heterogeneity[2, 14]. This is expressed through different approaches such as flow units[34], interstitial defects[35, 36], quasi-point defects (QPDs)[37] or liquid-like sites[38]. Here we will focus on the quasi-point defects theory, proposed by Perez et al.[37]. According to the QPD theory, the quasi-point defects in the glassy materials correspond to the fluctuation of the relevant physical magnitudes, namely energy, density, enthalpy and entropy, at nano-scale regions[37]. The concentration of defects

in the glassy materials presents a strong dependence on rejuvenation (i.e. plastic deformation[14]) and physical aging processes[39]. While defects annihilate during the physical aging below the glass transition temperature T_g, plastic deformation or other rejuvenation processes can enhance the concentration of defects[40]. In the framework of the QPD model, the evolution of the loss factor tanδ with temperature can be described as[37]:

$$\ln(\tan\delta) = -\frac{U_\beta}{k_B T} - \chi\ln(2\pi f) + \lambda \quad (3)$$

where U_β is the apparent activation energy of the structural relaxation, λ is a fitting parameter and χ is a correlation factor which is related to the concentration of defects, that is

χ = 0: fully ordered structure, corresponding to the ideal crystal. The movement of a structural unit depends on all other units.

χ = 1: fully disordered structure, corresponding to the ideal gas. The motion of a structural unit is fully independent of others units.

Fig. 6(a) displays the correlation between the double logarithmic plot of the loss factor tanδ and the angular frequency of the mechanical excitation ω of $Zr_{35}Hf_{17.5}Ti_{5.5}Al_{12.5}Co_{7.5}Ni_{12}Cu_{10}$ HEBMG at different temperatures. The correlation factor χ can be determined by the slope of the solid lines fitted by the equation (3). It can be seen that all the experimental data can be well described by the equation (3). **Fig. 6(b)** shows the evolution of the correlation factor χ with the temperature. According to the literature, the correlation factor χ ranges from 0.3 to 0.4 in typical MGs below the glass transition temperature T_g[1], where glasses are staying in an iso-configurational state. Interestingly, it must be noted that the correlation factor χ of $Zr_{35}Hf_{17.5}Ti_{5.5}Al_{12.5}Co_{7.5}Ni_{12}Cu_{10}$ HEBMG is significantly higher than 0.4 prior to the crystallization. According to the QPD model, it is reasonable to conclude that the configuration entropy of $Zr_{35}Hf_{17.5}Ti_{5.5}Al_{12.5}Co_{7.5}Ni_{12}Cu_{10}$ HEBMG is larger than that of typical MGs, reflecting a more disordered structure and higher concentration of quasi-point defects. When the temperature ranges between 695 K and 715 K, the glass system is no longer iso-configurational and χ increases by increasing the temperature. Above 715 K, the alloy is more stable due to the development of a crystalline phase. As a result, χ decreases reflecting a reduction of the concentration of defects. For the sake

of comparison, **Fig. 6(c)** shows the evolution of the correlation factor χ with the normalized temperature in typical Zr-based MGs. It can be seen that for temperatures between 0.96 T_g and T_g χ remains nearly constant, reflecting that the concentration of defects in the glass forming system remains almost constant below T_g. On the contrary, when the temperature surpasses T_g, χ increases due to the increase on the atomic mobility in the SLR.

As MGs are in an out-of-equilibrium state, physical aging below T_g drives the glass towards a more stable state. As a consequence, physical aging below T_g can tune the mechanical and physical properties of MGs[41, 42]. **Fig. 7** shows the evolution of the normalized storage modulus *E'/Eu* and the loss factor tanδ with isothermal aging time at different temperatures (i.e. 623, 638, 653 and 668 K, respectively). It should be noted that the physical and mechanical properties (enthalpy, density, shear modulus) change by increasing the aging time, as the glass evolves towards a more stable atomic configuration[43, 44]. In the studied alloy the storage modulus increases (as shown in **Fig. 7(a)**), and the loss factor decreases (as shown in **Fig. 7(b)**) by increasing the aging time. Previous experimental results suggested that the kinetic evolution of the physical properties during physical aging follows a similar tendency, which establishes a neat connection between the structural heterogeneity and the macroscopic properties of the glass[45, 46]. In addition to the effect of structural relaxation process on the mechanical properties, annealing induces also an increase in the shear modulus of MGs, which can be also determined by DMA. These observations confirm that MGs shift to a low-energy state during the physical aging process.

The kinetics of physical aging below T_g could be described by the empirical stretched exponential function in the form of the Kohlrausch-Williams-Watts (KWW)[47]:

$$\tan\delta(t=0) - \tan\delta(t_a) = A\left\{1 - \exp\left[-\left(\frac{t_a}{\tau}\right)^{\beta_{KWW}}\right]\right\} \quad (5)$$

where A is the maximum magnitude of the relaxation process, τ is the characteristic time of the relaxation and β_{KWW} is the stretching parameter, which ranges from 0 to 1. β_{KWW} can be used to describe the dynamic heterogeneity of the glassy solids[48, 49]. The value β_{KWW}=1 corresponds to a relaxation mechanism without any dynamic heterogeneity of the glassy solid. In addition, β_{KWW} is correlated to the fragility of the

glass, a parameter which actually reflects the deviation of both viscosity and relaxation time from the Arrhenius behavior[29]. The fitted values obtained for the $Zr_{35}Hf_{17.5}Ti_{5.5}Al_{12.5}Co_{7.5}Ni_{12}Cu_{10}$ HEBMG as aging temperature increases from 623 K to 688 K are $\beta_{KWW}(E'/Eu)$ = 0.50, 0.52, 0.54 and 0.47, respectively. On the other hand, from the analysis of the internal friction, i.e. tanδ, the values of $\beta_{KWW}(\tan\delta)$ at the same aging temperatures are $\beta_{KWW}(\tan\delta)$ = 0.54, 0.55, 0.55 and 0.58, respectively. These values reveal a broad relaxation time distribution which is related to the microstructural heterogeneity of $Zr_{35}Hf_{17.5}Ti_{5.5}Al_{12.5}Co_{7.5}Ni_{12}Cu_{10}$ HEBMG. Previous research proved that the parameter β_{KWW} measures the level of the cooperative rearrangement movement of the structural units[50]. Typically, the stretched parameter β_{KWW} in the "fragile" MGs is lower than 0.5, while that in the "strong" MGs is larger than 0.5[29]. In the current work, $\beta \gtrsim 0.5$, which indicates that the $Zr_{35}Hf_{17.5}Ti_{5.5}Al_{12.5}Co_{7.5}Ni_{12}Cu_{10}$ HEBMG is a moderately fragile glass former.

During the physical aging below the T_g, the aging intensity can be characterized by[47]:

$$\Delta = \frac{\tan\delta(t) - \tan\delta(t=\infty)}{\tan\delta(t=0) - \tan\delta(t=\infty)} \tag{6}$$

Fig. 8 shows the dependence of the double logarithm of the aging intensity parameter Δ on the logarithm of the aging time at different aging temperatures. The results present a pretty linear correlation. The value of slope confirmed by fitting is 0.51 for all curves and smaller than the stretched parameter β_{KWW}. Interestingly, Δ is independent of the aging temperature within this experimental temperature range, a result similar to that reported in one of the archetypical MGs, $Pd_{43}Ni_{10}Cu_{17}P_{20}$ [51].

The structural heterogeneity of MGs is the result of a wide distribution of deformation units[52]. As a consequence, the distribution of energy barriers of the deformation units is also broad. In the framework of the activation energy spectrum model, the evolution of the loss factor tanδ with aging time at a given aging temperature can be expressed as[53]:

$$\Delta\tan\delta(t) = \int_0^{+\infty} p(E_{app})\theta(E_{app}, T, t)dE_{app} \tag{7}$$

where $\Delta\tan\delta(t) = \tan\delta(t=0) - \tan\delta(t)$, $p(E_{app})$ is the activation energy spectrum during the relaxation process ranging from E_{app} to $E_{app}+dE_{app}$, and $\theta(E_{app}, T, t)$ is the characteristic aging function[53] :

$$\theta\left(E_{app},T,\mathrm{t}\right)=1-\exp\left[-\nu_{0}\mathrm{t}\exp\left(-\frac{E_{app}}{k_{B}T}\right)\right] \tag{8}$$

where ν_0 is the Debye frequency. In the isothermal structural relaxation, there is a critical activation energy E_{cri}. Only the structural units with energy barrier $E_{app}<E_{cri}$ participate in the structural relaxation. On a step-like approximation, $p(E_{app})$ can be obtained as[43, 54]:

$$p\left(E_{app}\right)=\frac{-1}{k_{B}T}\frac{\mathrm{d}\tan\delta}{\mathrm{d}\left(\ln\mathrm{t}\right)} \tag{9}$$

and the energy can be derived from the Arrhenius equation:

$$E_{app}=k_{B}T\ln\left(\nu_{0}\mathrm{t}\right) \tag{10}$$

Fig. 9 exhibits the temperature dependence of activation energy spectra $P(E_{app})$ of $Zr_{35}Hf_{17.5}Ti_{5.5}Al_{12.5}Co_{7.5}Ni_{12}Cu_{10}$ HEBMG, where $P(E_{app})$ is normalized by its maximum value. The shape of the spectra is similar to the Gaussian distribution of stress relaxation in MGs[55]. By increasing the temperature, the spectra shifts toward higher values, reflecting that defects of higher activation energy can be activated in the relaxation process. This fact shows the effect on annealing in the structural relaxation: during the heating process, structural units with low activation energies are relaxed, reducing the concentration of quasi-point defects and the structural heterogeneity. The subsequent process of mechanical relaxation acts on the higher activation energy, yet unrelaxed structural units.

As discussed above, physical aging below the T_g modifies the physical and mechanical properties of MGs. **Fig. 10** shows the evolution of the loss factor tanδ with temperature at different states, i.e., as cast and physically aged at different temperatures for 12 hours, of the $Zr_{35}Hf_{17.5}Ti_{5.5}Al_{12.5}Co_{7.5}Ni_{12}Cu_{10}$ HEBMG. The intensity of the loss factor tanδ decreases by increasing the aging temperature of the samples. It can be seen from **Fig. 10** that the "excess wing" process is less evident after physical aging below T_g. As mentioned above, the loss factor tanδ is related to the mobility of the atoms or molecules. The reduction of tanδ corresponds to the decrease of the atomic mobility of MGs, showing that the glassy solids shift to a more stable state on annealing. On the contrary, rejuvenation improves the atomic mobility and enhances the plasticity of MGs[40, 56]. Unlike Zr-based MGs, La-based MGs exhibit a pronounced β relaxation peak in the loss factor[57]. Compared with the as-cast state, physical aging below the

T_g induces a reduction of the intensity of β relaxation. But such heat treatments are incapable of suppressing β relaxation. The influence of the chemical compositions on the intensity of the β relaxation in MGs is still an unsolved question.

4. Conclusions

In the current research, dynamic mechanical properties of $Zr_{35}Hf_{17.5}Ti_{5.5}Al_{12.5}Co_{7.5}Ni_{12}Cu_{10}$ non-equiatomic HEBMG were investigated by dynamic mechanical spectroscopy. The main results are summarized as follows:

- From the mechanical spectra, the $Zr_{35}Hf_{17.5}Ti_{5.5}Al_{12.5}Co_{7.5}Ni_{12}Cu_{10}$ HEBMG presents a typical excess wing-type β relaxation process.
- The dynamic mechanical behavior of $Zr_{35}Hf_{17.5}Ti_{5.5}Al_{12.5}Co_{7.5}Ni_{12}Cu_{10}$ HEBMG was analyzed in the framework of the QPD theory. The correlation factor χ of $Zr_{35}Hf_{17.5}Ti_{5.5}Al_{12.5}Co_{7.5}Ni_{12}Cu_{10}$ HEBMG below the glass transition temperature was obtained, showing a value higher than that of conventional MGs. This phenomenon is ascribed to the fact that the configuration entropy of $Zr_{35}Hf_{17.5}Ti_{5.5}Al_{12.5}Co_{7.5}Ni_{12}Cu_{10}$ HEBMG is larger than typical MGs, consequence of a more disordered structure and a higher "defect" concentration.
- Physical aging below the glass transition temperature T_g leads to a reduction of the concentration of defects of $Zr_{35}Hf_{17.5}Ti_{5.5}Al_{12.5}Co_{7.5}Ni_{12}Cu_{10}$ HEBMG, as observed in the computed activation energy spectra.
- The $Zr_{35}Hf_{17.5}Ti_{5.5}Al_{12.5}Co_{7.5}Ni_{12}Cu_{10}$ HEBMG shows most of the dynamic features of Zr/Hf-based MGs, despite the excess of configurational entropy.

Acknowledgements

This work is supported by the NSFC (Grant No. 51971178), the Fundamental Research Funds for the Central Universities (Nos. 3102019ghxm007 and 3102017JC01003), Astronautics Supporting Technology Foundation of China (2019-HT-XG) and the Natural Science Foundation of Shaanxi Province (No. 2019JM-344). D.C. and E.P. acknowledge the financial support from MINECO (grant FIS2017-82625-P) and Generalitat de Catalunya (grant 2017SGR0042).

References

[1] J.C. Qiao, J.M. Pelletier, *Journal of Materials Science & Technology*, 30 (2014) 523-545.

[2] W.H. Wang, *Progress in Materials Science*, 106 (2019) 100561.

[3] Y.J. Huang, Z.L. Ning, Z. Shen, W.Z. Liang, H.C. Sun, J.F. Sun, *Journal of Materials Science & Technology*, 33 (2017) 1153-1158.

[4] B.A. Sun, W.H. Wang, *Progress in Materials Science*, 74 (2015) 211-307.

[5] X.Q. Gao, K. Zhao, H.B. Ke, D.W. Ding, W.H. Wang, H.Y. Bai, *Journal of Non-Crystalline Solids*, 357 (2011) 3557-3560.

[6] Z. Yong, T.T. Zuo, T. Zhi, M.C. Gao, K.A. Dahmen, P.K. Liaw, P.L. Zhao, *Progress in Materials Science*, 61 (2014) 1-93.

[7] H. Ding, Y. Shao, P. Gong, J. Li, K. Yao, *Materials letters*, 125 (2014) 151-153.

[8] A. Takeuchi, N. Chen, T. Wada, Y. Yokoyama, H. Kato, A. Inoue, J.W. Yeh, *Intermetallics*, 19 (2011) 1546-1554.

[9] H. Li, X. Xie, K. Zhao, Y. Wang, Y. Zheng, W. Wang, L. Qin, *Acta Biomaterialia*, 9 (2013) 8561-8573.

[10] J.-W. Yeh, *Jom*, 65 (2013) 1759-1771.

[11] R. Wei, J. Tao, H. Sun, C. Chen, G.W. Sun, F.S. Li, *Materials Letters*, 197 (2017) 87-89.

[12] T. Wada, J. Jiang, K. Yubuta, H. Kato, A. Takeuchi, *Materialia*, 7 (2019) 100372.

[13] W.H. Wang, *Progress in Physics*, 33 (2013) 177-351.

[14] J.C. Qiao, Q. Wang, J.M. Pelletier, H. Kato, R. Casalini, D. Crespo, E. Pineda, Y. Yao, Y. Yang, *Progress in Materials Science*, 104 (2019) 250-329.

[15] C.A. Angell, K.L. Ngai, G.B. McKenna, P.F. McMillan, S.W. Martin, *Journal of Applied Physics*, 88 (2000) 3113-3157.

[16] H.B. Yu, W.H. Wang, H.Y. Bai, K. Samwer, *National Science Review*, 1 (2014) 429-461.

[17] M. Yang, X.J. Liu, Y. Wu, H. Wang, S.H. Jiang, X.Z. Wang, Z.P. Lv, *Scientia Sinica Physica, Mechanica & Astronomica*, 50 (2020) 067003.

[18] J.C. Qiao, J.M. Pelletier, N. Li, Y. Yao, *Journal of Iron and Steel Research International*, 23 (2016) 19-23.

[19] W. Jiang, B. Zhang, *Journal of Applied Physics*, 127 (2020) 115104.

[20] P. Gong, S. Zhao, H. Ding, K. Yao, X. Wang, *Journal of Materials Research*, 30 (2015) 2772-2782.

[21] Q. Zhou, Y. Du, W. Han, Y. Ren, H. Zhai, H. Wang, *Scripta Materialia*, 164 (2019) 121-125.

[22] E. Pineda, P. Bruna, B. Ruta, M. Gonzalez-Silveira, D. Crespo, *Acta Materialia*, 61 (2013) 3002-3011.

[23] T.G. Nieh, J. Wadsworth, *Scripta Materialia*, 54 (2006) 387-392.

[24] Y. Kawamura, T. Nakamura, H. Kato, H. Mano, A. Inoue, *Materials Science and Engineering A*, 304 (2001) 674-678.

[25] G.P. Johari, M. Goldstein, *The Journal of Chemical Physics*, 53 (1970) 2372-2388.

[26] K. Ngai, Relaxation and diffusion in complex systems, *Springer Science & Business Media*, 2011.

[27] Q. Wang, J. Liu, Y. Ye, T. Liu, S. Wang, C. Liu, J. Lu, Y. Yang, *Materials Today*, 20 (2017) 293-300.

[28] W.H. Wang, *Progress in Materials Science*, 57 (2012) 487-656.

[29] R. BoHmer, K.L. Ngai, C.A. Angell, D.J. Plazek, *Journal of Chemical Physics*, 99 (1993) 4201-4209.

[30] Q. Hao, W.Y. Jia, J.C. Qiao, *Journal of Non-Crystalline Solids*, 546 (2020) 120266.

[31] J.C. Qiao, J.M. Pelletier, H.C. Kou, X. Zhou, *Intermetallics*, 28 (2012) 128-137.

[32] Y.H. Liu, D. Wang, K. Nakajima, W. Zhang, A. Hirata, T. Nishi, A. Inoue, M.W. Chen, *Physical Review Letters*, 106 (2011) 125504.

[33] H. Wagner, D. Bedorf, S. Küchemann, M. Schwabe, B. Zhang, W. Arnold, K. Samwer, *Nature Materials*, 10 (2011) 439-442.

[34] W.H. Wang, *Scientia Sinica Physica,Mechanica & Astronomica*, 44 (2014) 396-405.

[35] V.A. Khonik, *Chinese Physics B*, 26 (2017) 20-31.

[36] Q. Hao, J.C. Qiao, E. Goncharova, G. Afonin, M.N. Liu, Y.T. Cheng, V. Khonik, *Chinese Physics B*, 29 (2020) 086402.

[37] J. Perez, *Solid State Ionics*, 39 (1990) 69-79.

[38] T. Egami, *Progress in Materials Science*, 56 (2011) 637-653.

[39] J.M. Pelletier, D.V. Louzguine-Luzgin, S. Li, A. Inoue, *Acta Materialia*, 59 (2011) 2797-2806.

[40] J.C. Qiao, J.M. Pelletier, C. Esnouf, Y.H. Liu, H. Kato, *Journal of Alloys and Compounds*, 607 (2014) 139-149.

[41] I.M. Hodge, *Ence*, 267 (1995) 1945-1947.

[42] D. Cangialosi, V.M. Boucher, A. Alegria, J. Colmenero, *Soft Matter*, 9 (2013) 8619-8630.

[43] S.V. Khonik, A.V. Granato, D.M. Joncich, A. Pompe, V.A. Khonik, *Physical Review Letters*, 100 (2008) 065501.

[44] T. Zhang, F. Ye, Y. Wang, J. Lin, *Metallurgical and Materials Transactions A*, 39 (2008) 1953-1957.

[45] J. Ye, J. Lu, C. Liu, Q. Wang, Y. Yang, *Nature Materials*, 9 (2010) 619-623.

[46] J. Ding, Y. Cheng, H. Sheng, M. Asta, R.O. Ritchie, E. Ma, *Nature Communications*, 7 (2016) 1-10.

[47] J.C. Qiao, J.M. Pelletier, *Intermetallics*, 28 (2012) 40-44.

[48] P. Zhang, J.J. Maldonis, Z. Liu, J. Schroers, P.M. Voyles, *Nature Communications*, 9 (2018) 1-7.

[49] M. Atzmon, *Journal of Applied Physics*, 123 (2018) 065103.

[50] Ian, M., Hodge, G., S., Huvard, *Macromolecules*, 16 (1983) 371-375.

[51] X.B. Wu, L.J. Guo, C.S. Liu, *Journal of Applied Physics*, 115 (2014) 223506.

[52] J.C. Ye, J. Lu, C.T. Liu, Q. Wang, Y. Yang, *Nature Materials*, 9 (2010) 619-623.

[53] M.R.J. Gibbs, J.E. Evetts, J.A. Leake, *Journal of Materials Science*, 18 (1983) 278-288.

[54] W. Dmowski, T. Iwashita, C.P. Chuang, J. Aimer, T. Egami, *Physical Review Letters*, 105 (2010) 205502.

[55] W. Jiao, P. Wen, H.L. Peng, H.Y. Bai, B.A. Sun, W.H. Wang, *Applied Physics Letters*, 102 (2013) 101903.

[56] J.L. Gu, H.W. Luan, S.F. Zhao, H.T. Bu, K.F. Yao, *Materials Science and Engineering A*, 786 (2020) 139417.

[57] J.C. Qiao, Y.H. Chen, R. Casalini, J.M. Pelletier, Y. Yao, *Journal of Materials Science & Technology*, 35 (2019) 982-986.

[58] W.H. Wang, *Journal of Applied Physics*, 110 (2011) 053521.

[59] J.C. Qiao, R. Casalini, J.M. Pelletier, Y. Yao, *Journal of Non Crystalline Solids*, 447 (2016) 85-90.

[60] J.C. Qiao, Y.X. Chen, J.M. Pelletier, H. Kato, D. Crespo, Y. Yao, V.A. Khonik, *Materials Science and Engineering A*, 719 (2018) 164-170.

[61] J.C. Qiao, J. Cong, Q. Wang, J.M. Pelletier, *Journal of Alloys and Compounds*, 749 (2018) 262-267.

Captions of the Figures and Tables

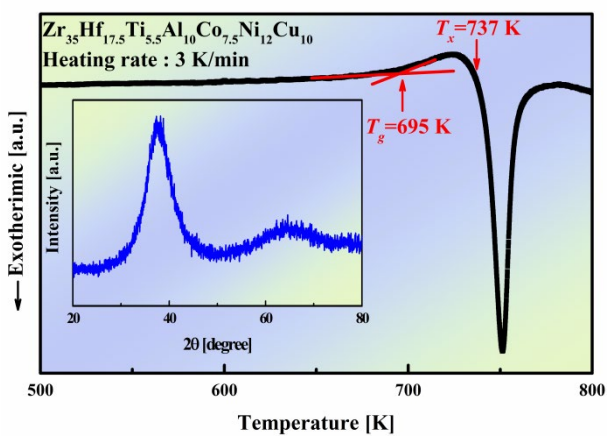

Fig. 1. DSC curve of $Zr_{35}Hf_{17.5}Ti_{5.5}Al_{12.5}Co_{7.5}Ni_{12}Cu_{10}$ high entropy bulk metallic glass (heating rate is 3 K/min). Inset is the XRD pattern of $Zr_{35}Hf_{17.5}Ti_{5.5}Al_{12.5}Co_{7.5}Ni_{12}Cu_{10}$ high entropy bulk metallic glass.

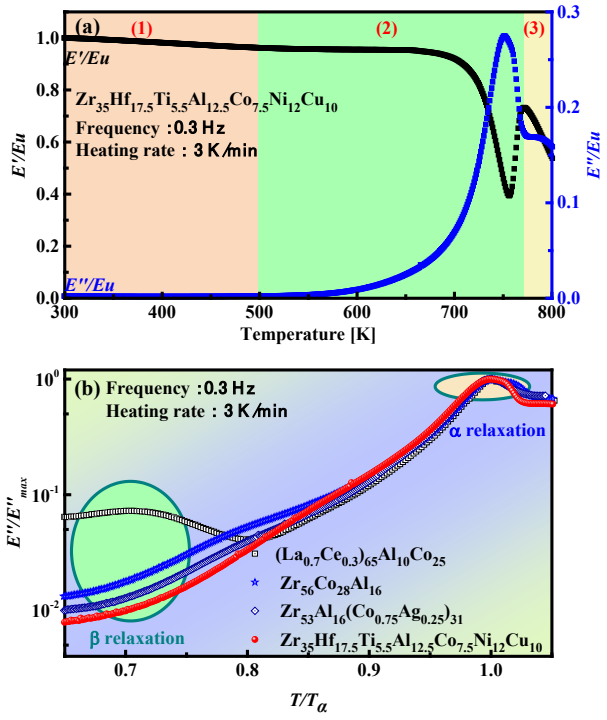

Fig. 2. (a)Temperature dependence of the normalized storage modulus and the loss modulus of $Zr_{35}Hf_{17.5}Ti_{5.5}Al_{12.5}Co_{7.5}Ni_{12}Cu_{10}$ high entropy bulk metallic glass. (b)The normalized loss mudulus E''/E''_{max} in typical MGs as a function of the normalized temperature T/T_{α}. E''_{max} is the maximum of the loss modulus. T_{α} is the peak temperature of the main α relaxation.

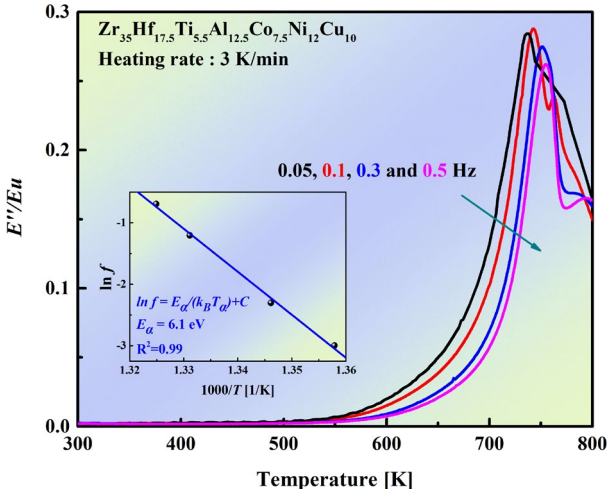

490

491 **Fig. 3.** Temperature dependence of the normalized loss modulus of
492 $Zr_{35}Hf_{17.5}Ti_{5.5}Al_{12.5}Co_{7.5}Ni_{12}Cu_{10}$ high entropy bulk metallic glass with different driving
493 frequencies (0.05, 0.1, 0.3 and 0.5 Hz). The heating rate is 3 K/min. Inset shows ln$f$ as
494 a function of 1000/T_α.

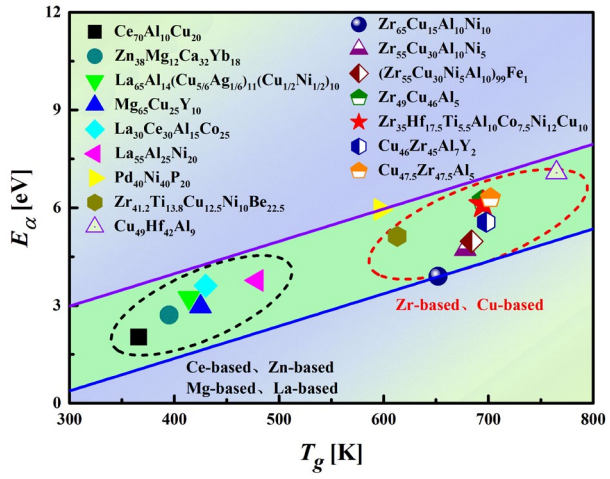

495

496 **Fig. 4.** The activation energy of the main α relaxation E_α *versus* the glass transition
497 temperature T_g in typical MGs.

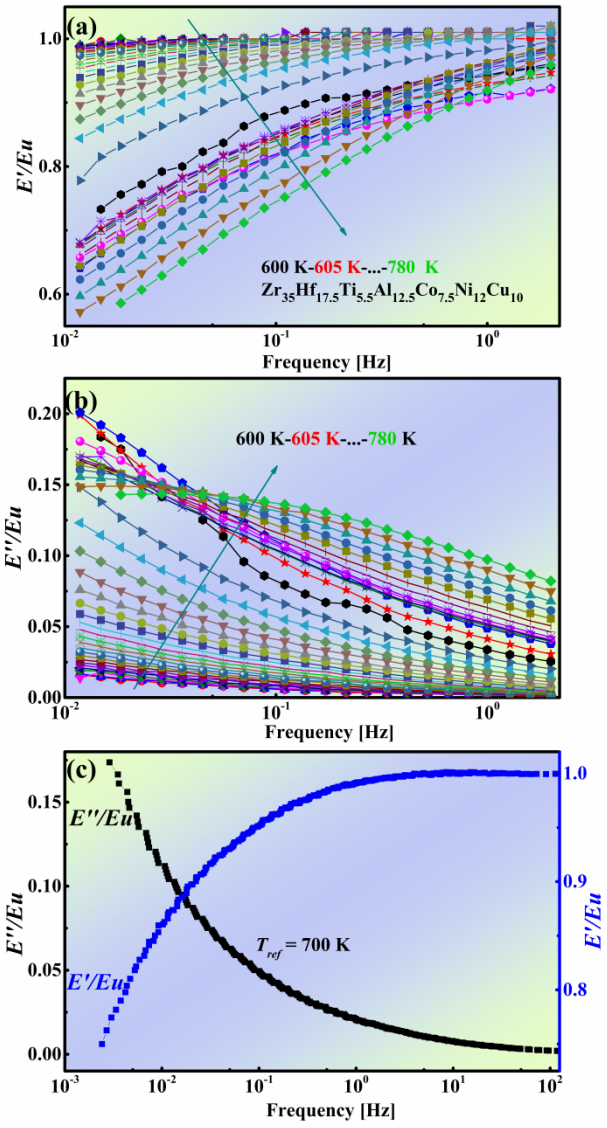

498

499 **Fig. 5.** Dependence of the normalized storage E'/E_u (a) and the loss modulus E''/E_u (b)
500 on frequency at different temperatures of $Zr_{35}Hf_{17.5}Ti_{5.5}Al_{12.5}Co_{7.5}Ni_{12}Cu_{10}$ high entropy
501 bulk metallic glass. (c)Master curve of the normalized storage modulus E'/E_u and the
502 loss modulus E''/E_u with the frequency. The reference temperature is 700 K.

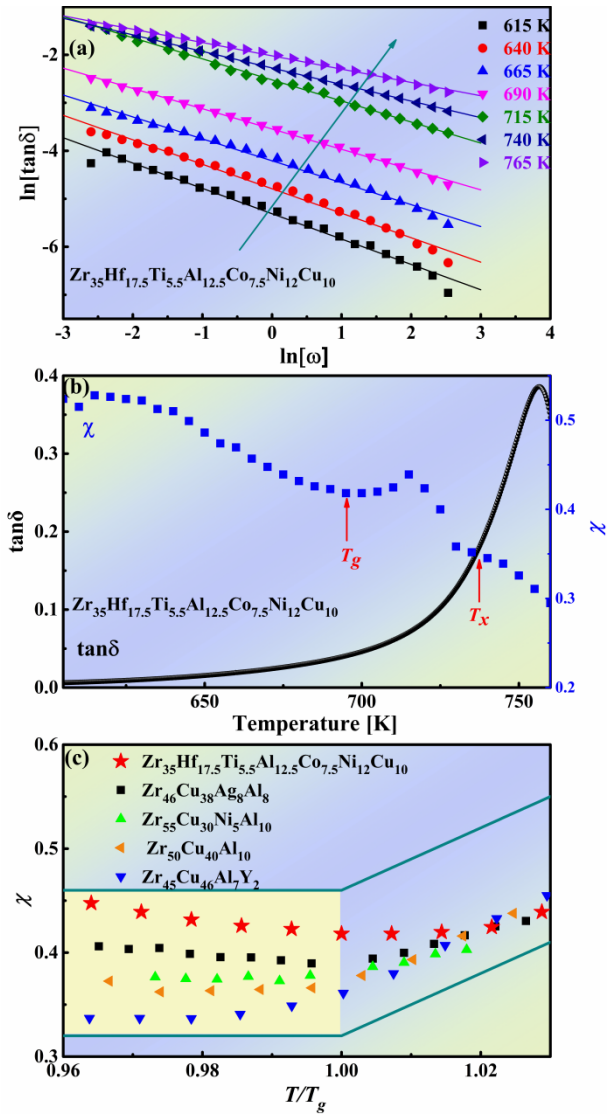

503

504 **Fig. 6.** (a)The loss factor tanδ varies with the driving frequency at various temperature
505 of $Zr_{35}Hf_{17.5}Ti_{5.5}Al_{12.5}Co_{7.5}Ni_{12}Cu_{10}$ high entropy bulk metallic glass. Solid lines are the
506 best fits by the equation (3). (b)Evolution of the correlation factor χ and loss factor tanδ
507 with temperature of $Zr_{35}Hf_{17.5}Ti_{5.5}Al_{12.5}Co_{7.5}Ni_{12}Cu_{10}$ high entropy bulk metallic glass.
508 (c)Evolution of the correlation factor χ with the normalized temperature in typical MGs.

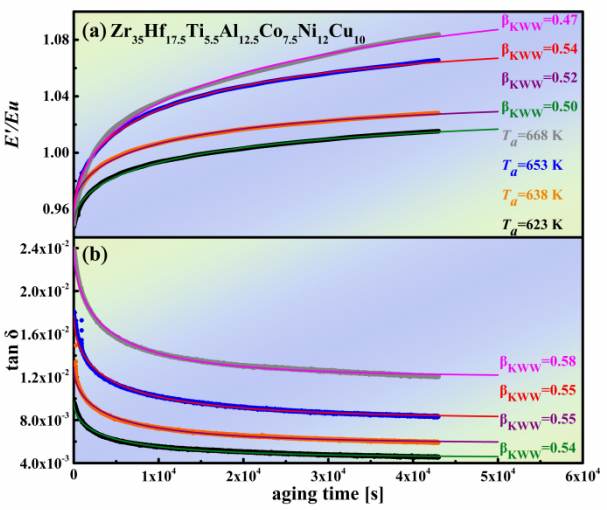

Fig. 7. Evolution of the storage modulus *E'/Eu* (a) and loss factor tanδ (b) with the aging time at different aging temperatures of $Zr_{35}Hf_{17.5}Ti_{5.5}Al_{12.5}Co_{7.5}Ni_{12}Cu_{10}$ high entropy bulk metallic glass. The aging temperatures are 623, 638, 653 and 668 K, respectively. The solid lines are fitted by the equation (5).

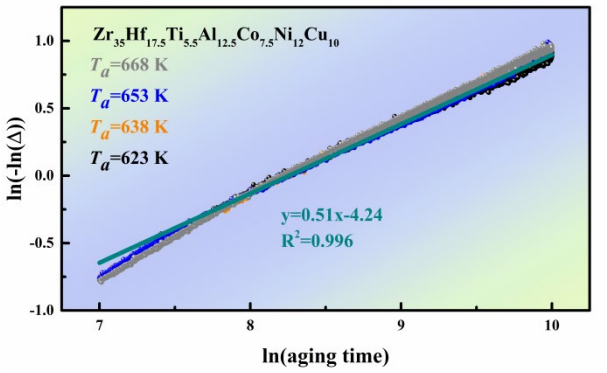

Fig. 8. Double logarithm of the loss factor tanδ vs the logarithm of the aging time at different aging temperatures for $Zr_{35}Hf_{17.5}Ti_{5.5}Al_{12.5}Co_{7.5}Ni_{12}Cu_{10}$ high entropy bulk metallic glass.

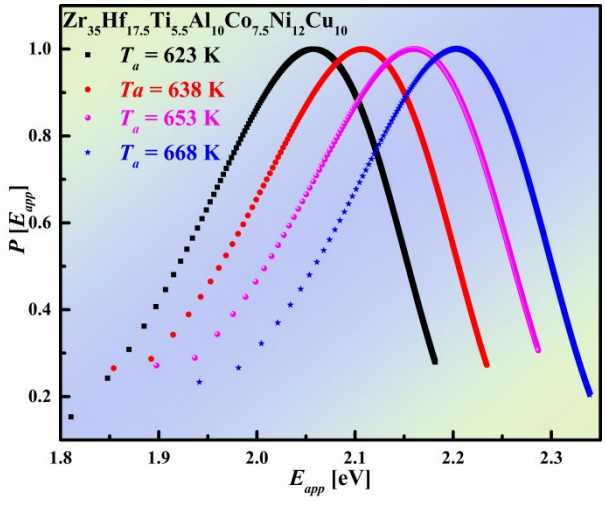

Fig. 9. Temperature dependence of normalized activation energy spectra $P(E_{app})$ of $Zr_{35}Hf_{17.5}Ti_{5.5}Al_{12.5}Co_{7.5}Ni_{12}Cu_{10}$ high entropy bulk metallic glass.

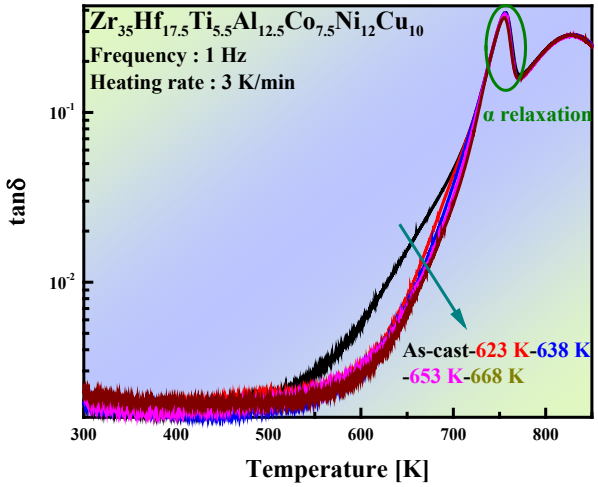

Fig. 10. Evolution of the loss factor tanδ with temperature of $Zr_{35}Hf_{17.5}Ti_{5.5}Al_{12.5}Co_{7.5}Ni_{12}Cu_{10}$ high entropy bulk metallic glass at different states: as-cast state and the samples were annealed at different temperatures, i.e., 623, 638, 653 and 668 K, for 12 hours.

534 **Table 1** Activation energy of the main α relaxation in typical MGs obtained by DMA
535 technique.

Metallic glasses	T_g [K]	E_α [eV]	Reference
$Ce_{70}Al_{10}Cu_{20}$	366	2.03	[58]
$Zn_{38}Mg_{12}Ca_{32}Yb_{18}$	395	2.71	[59]
$La_{65}Al_{14}(Cu_{5/6}Ag_{1/6})_{11}(Cu_{1/2}Ni_{1/2})_{10}$	414	3.24	[60]
$Mg_{65}Cu_{25}Y_{10}$	425	2.97	[58]
$La_{30}Ce_{30}Al_{15}Co_{25}$	430	3.61	[57]
$La_{55}Al_{25}Ni_{20}$	479	3.77	[58]
$Pd_{40}Ni_{40}P_{20}$	597	5.95	[58]
$Zr_{41.2}Ti_{13.8}Cu_{12.5}Ni_{10}Be_{22.5}$	613	5.13	[58]
$Zr_{65}Cu_{15}Al_{10}Ni_{10}$	652	3.90	[58]
$Zr_{55}Cu_{30}Al_{10}Ni_5$	678	4.73	[58]
$(Zr_{55}Cu_{30}Ni_5Al_{10})_{99}Fe_1$	684	4.97	[61]
$Zr_{49}Cu_{46}Al_5$	694	6.22	[58]
$Zr_{35}Hf_{17.5}Ti_{5.5}Al_{12.5}Co_{7.5}Ni_{12}Cu_{10}$	695	6.10	current work
$Cu_{46}Zr_{45}Al_7Y_2$	698	5.56	[58]
$Zr_{47.5}Cu_{47.5}Al_5$	702	6.30	[58]
$Cu_{49}Hf_{42}Al_9$	765	7.08	current work

536